JOURNAL OF MATERIALS SCIENCE 35 (2000) 4177–4183

Unusual dysprosium ceramic nano-fiber growth in a supercritical aqueous solution

M. M. HOFFMANN, J. S. YOUNG, J. L. FULTON*
Environmental and Health Sciences Division, Pacific Northwest National Laboratory, PO Box 999 MS P8-19, Richland, Washington 99352, USA
E-mail: jl_fulton@pnl.gov

The formation of nano-size ceramic fibers having diameters as small as 20 nm is described. This material was obtained by a simple precipitation reaction from a supercritical aqueous dysprosium bromide solution at high temperatures (450°C). The nano-structures have unusually high structural stability for extended time periods in this extreme solvent environment. The experimental procedures are described and analysis of the materials by scanning and transition electron microscopy, and x-ray diffraction is presented. The new materials may have useful applications as high-strength, corrosion resistant materials or as stable catalyst supports for extreme conditions.

1. Introduction

The slow hydrothermal growth of single crystals is a well-established technique that has been used for decades in the production of materials such as single crystal quartz. It is however not a technique that is usually used to generate particles with dimensions in the nanometer size range. In particular, at temperatures and pressures exceeding those at the critical point of pure water ($T_c = 374$°C, $P_c = 221$ bar, $\rho_c = 0.322$ g/cm^3) the production of nano-particles becomes more difficult in a static cell. At these conditions, the solubilities of ceramics such as SiO_2 or Al_2O_3 are appreciable, and the rates of crystal growth and Ostwald ripening are high. Furthermore, the kinetics of chemical reactions in a single phase are expected to be fast. Hence, nanometer-sized particles have so far only been obtained from a supercritical aqueous environment by two types of non-equilibrium processes. The first approach is to establish a short residence time to limit crystal growth by inducing an abrupt homogeneous nucleation of a dissolved solute in the region of an expanding jet. This approach is accomplished in the RESS process (rapid expansion of supercritical fluid solutions) [1, 2] and in the case of reacting precursor compounds in the short thermal cycle of the RTDS process (rapid thermal decomposition of precursors in solution) [3–7]. The second widely used non-equilibrium approach for production of nano-particles employs a solid component as one of the reacting starting materials whereby the rate of dissolution limits the precipitation. Typical temperatures for this method range between the boiling and the critical point of water whereas pressures are typically just above the vapor pressure. The literature concerning this approach has been reviewed [8, 9]. Fibrous materials were also obtained by this hydrothermal process at temperatures exceeding the critical temperature of pure water in the case of various titanates [10, 11] and amphiboles [12]. Finally, at subcritical temperatures (200°C), whiskers of hydroxyapatite with widths of 0.1 to 1 μm were obtained from a dilute (at room temperature single-phased) solution of beta-$Ca_3(PO_4)_2$ near the vapor pressure of the solution [13].

Here we report the unusual formation of nanometer-sized ceramic fibers from a supercritical aqueous solution containing dysprosium bromide and dilute sodium fluoride. The obtained fibers have diameters as small as 20 nm. The unusual aspects of this observation are a) that the nano-sized structures appear to be *stable* in a supercritical water environment over prolonged times and b) that the materials were obtained from a precipitation reaction from a solution that started out in a single phase at room temperature.

2. Experimental procedure

The samples were synthesized in a high-pressure cell made from Hastelloy C-22. Sample solutions can be introduced into the cell through feed lines made from a titanium alloy. The internal volume of this cell is approximately 5 ml. The cell was heated with cartridge heaters and the temperature was controlled to an accuracy of ±3°C using a three-mode controller (Omega, No. CN3000). As a general safety measure, an additional redundant temperature limit controller (Watlow, Series 94) was placed in series with the three-mode temperature controller. Pressure was applied using a standard syringe pump (ISCO Model 100DX), and the system's pressure was monitored to within ±1 bar with a calibrated electronic transducer (Precise Sensors. No. D451).

The chemicals were obtained from Aldrich and were used as received. Double distilled water was used for

* Author to whom all correspondence should be addressed.

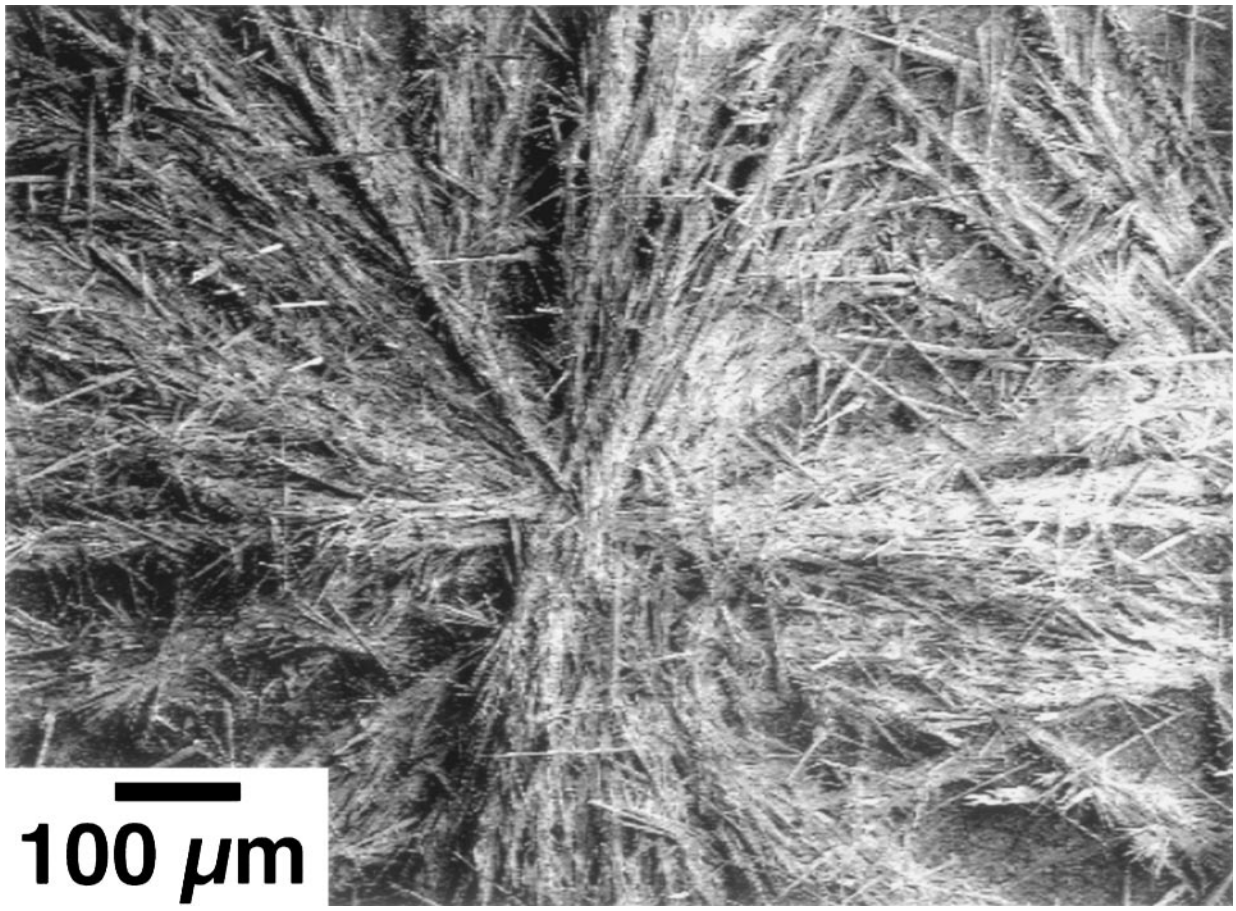

(a)

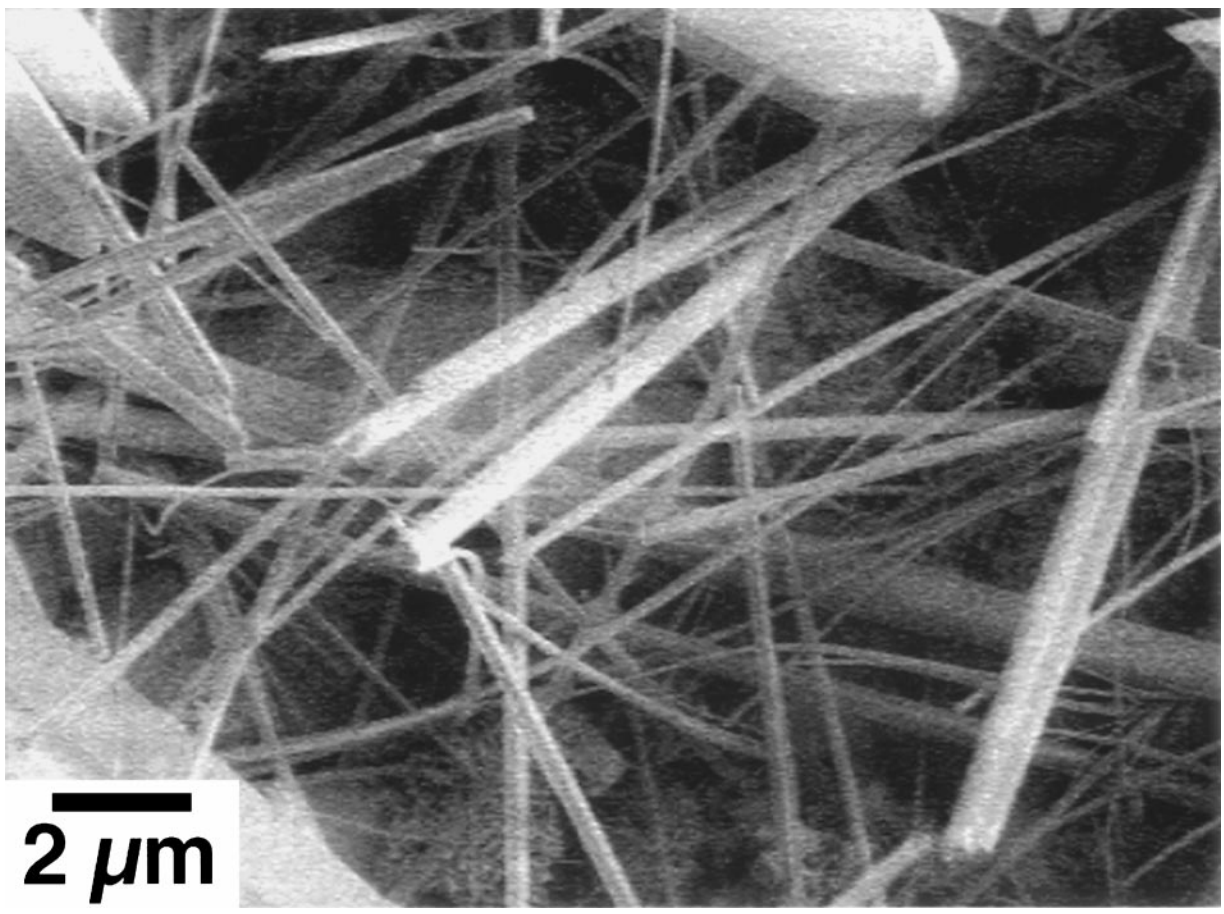

(b)

Figure 1 SEM micrographs of dysprosium ceramic fiber sample 1, a) at low magnification showing the large-scale star-like structural order, b) at higher magnification revealing the presence of fibers that are polydispersed in diameters and a second solid phase of long platelets, c) high magnification view of a fiber of approximately 50 nm in diameter that is located in front of a larger fiber that is 300 nm in diameter. (*Continued*)

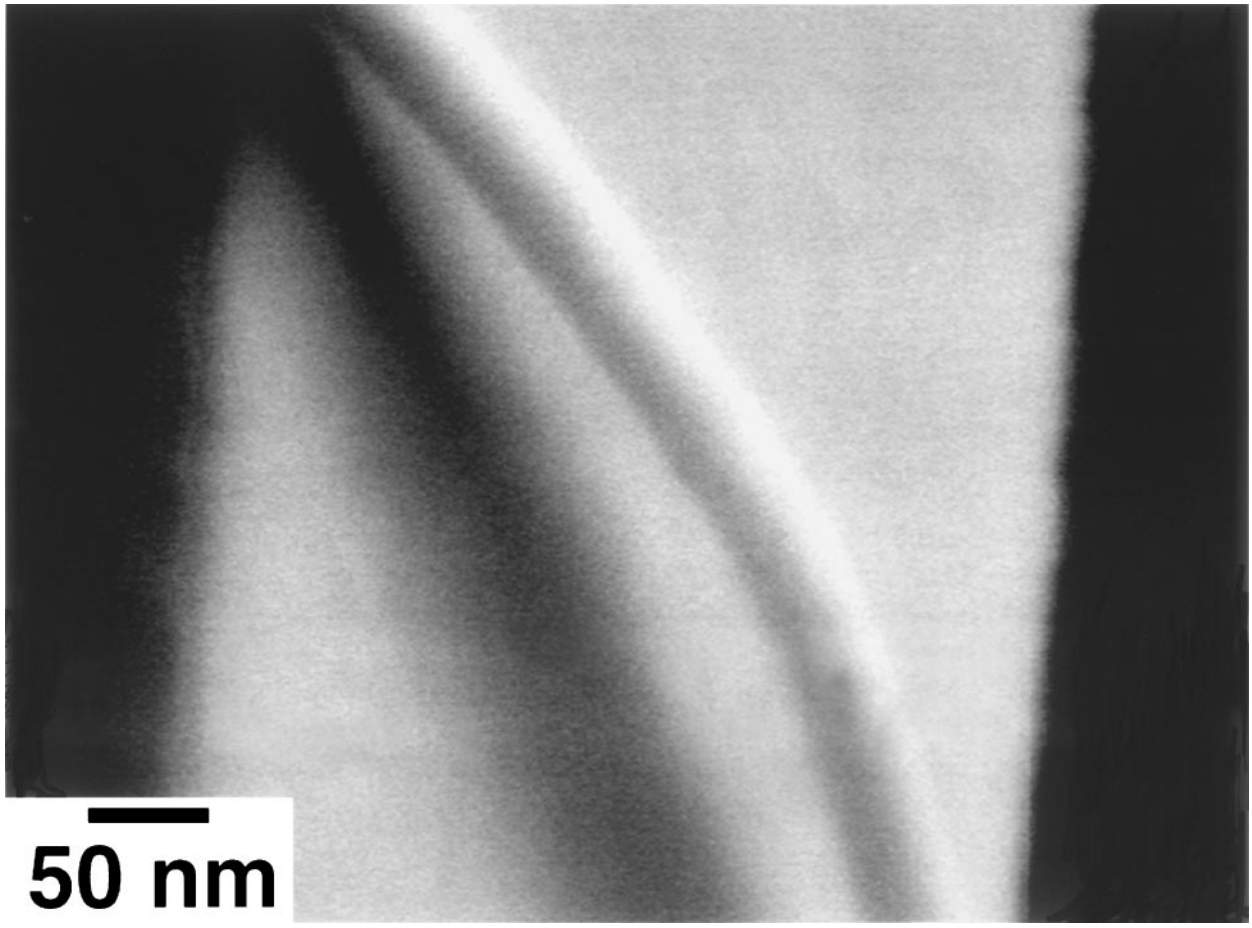

(c)

Figure 1 (*Continued*).

all experiments. Further details on experimental procedures are provided with the description of the dysprosium samples in the results and discussion section.

Scanning electron microscopy (SEM) analysis was carried out with a LEO 982 Field Emission Scanning Electron Microscope equipped with a SiLi detector of 128 eV resolution and with an Oxford ISIS energy dispersive x-ray microanalysis system. The transmission electron microscope (TEM) was equipped with a field-emission gun (FEG) and a energy dispersive x-ray spectrometer (EDS) system which allows compositional analysis with a 0.7 nm FWHM probe size (beam current = 0.25 nA).

3. Results and discussion

3.1. Production of dysprosium ceramic nano-fibers

Two different nano-fiber samples were produced. Sample 1 was produced from a solution that contained a small amount of fluoride. A 0.2 m $DyBr_3$/0.02 m NaF solution was heated to 450°C at 450 bar pressure in the high-pressure cell. After 3 hours, 10 ml of a 0.01 molal NaF solution was flushed through the cell. Temperature and pressure were then maintained for another 17 hours before the cell was allowed to cool down to room temperature. This procedure yielded a white fibrous precipitate of which three SEM micrographs are shown in Fig. 1. The lowest magnification SEM micrograph in Fig. 1a demonstrates the fibrous character of the sample. The fibers are aggregated to produce a large-scale star-like structural order. The higher magnification of Fig. 1b typifies the polydispersity in the fiber diameters and reveals that a second solid phase having a long platelet morphology is also present in this sample. While most of the fibers have diameters

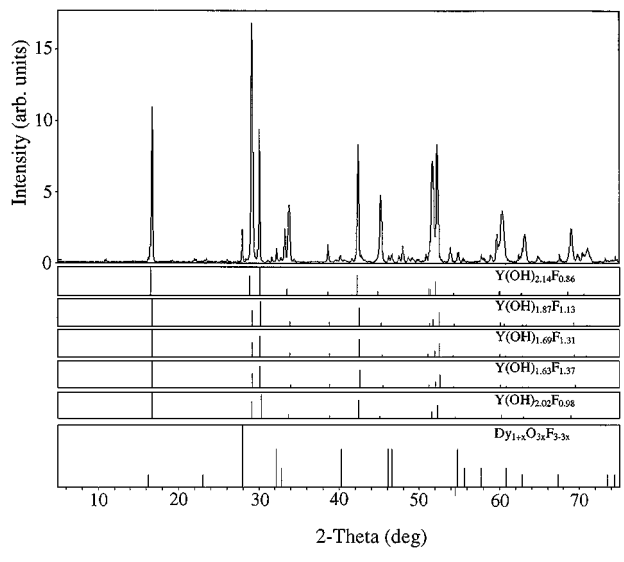

Figure 2 XRD with phase identification of sample 1. The major phase of Sample 1 is isomorph to a hexagonal yttrium hydroxide fluoride structure of space group $P6_3/m$. A minor phase is identified as $Dy_{1+x}O_{3x}F_{3(1-x)}$.

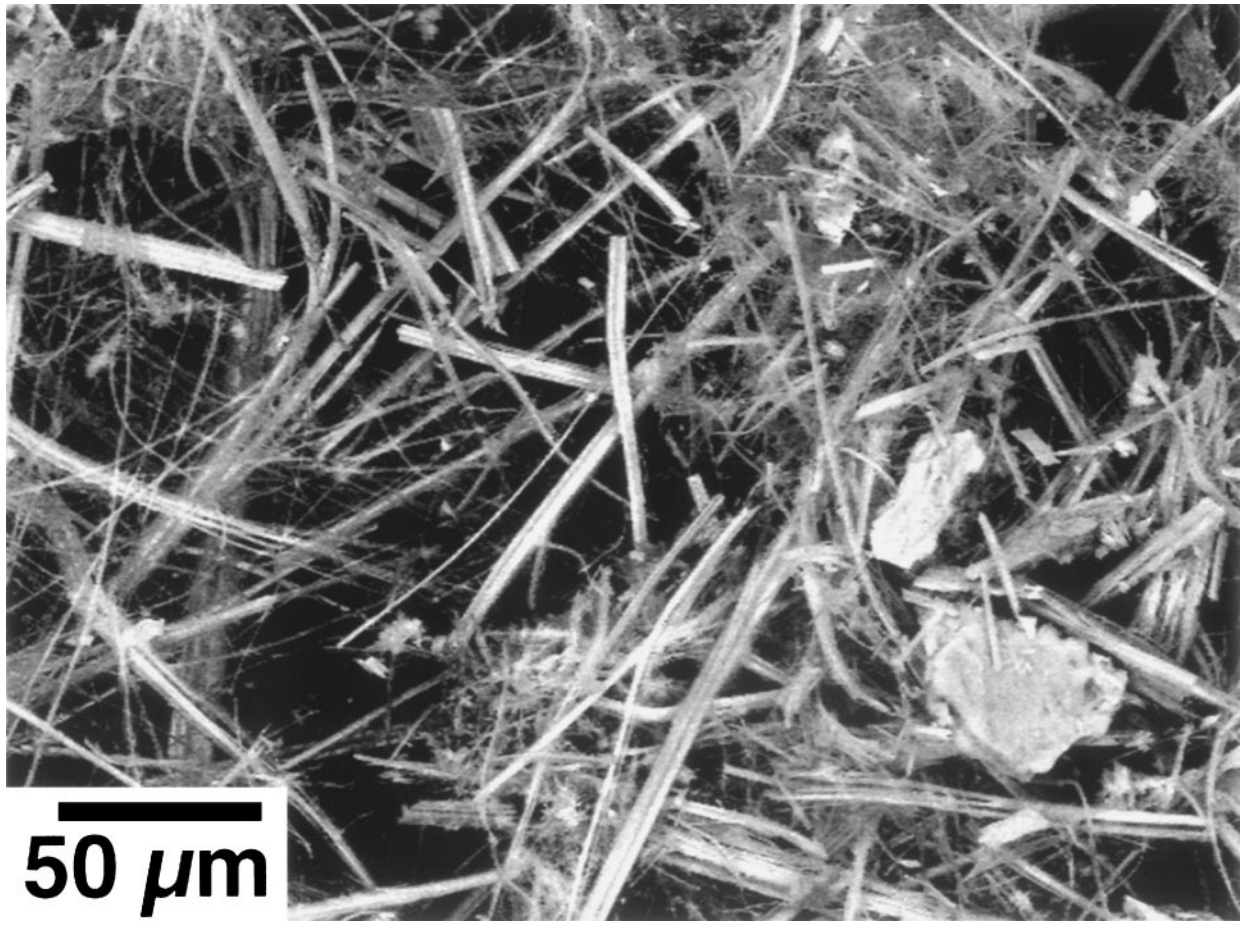

(a)

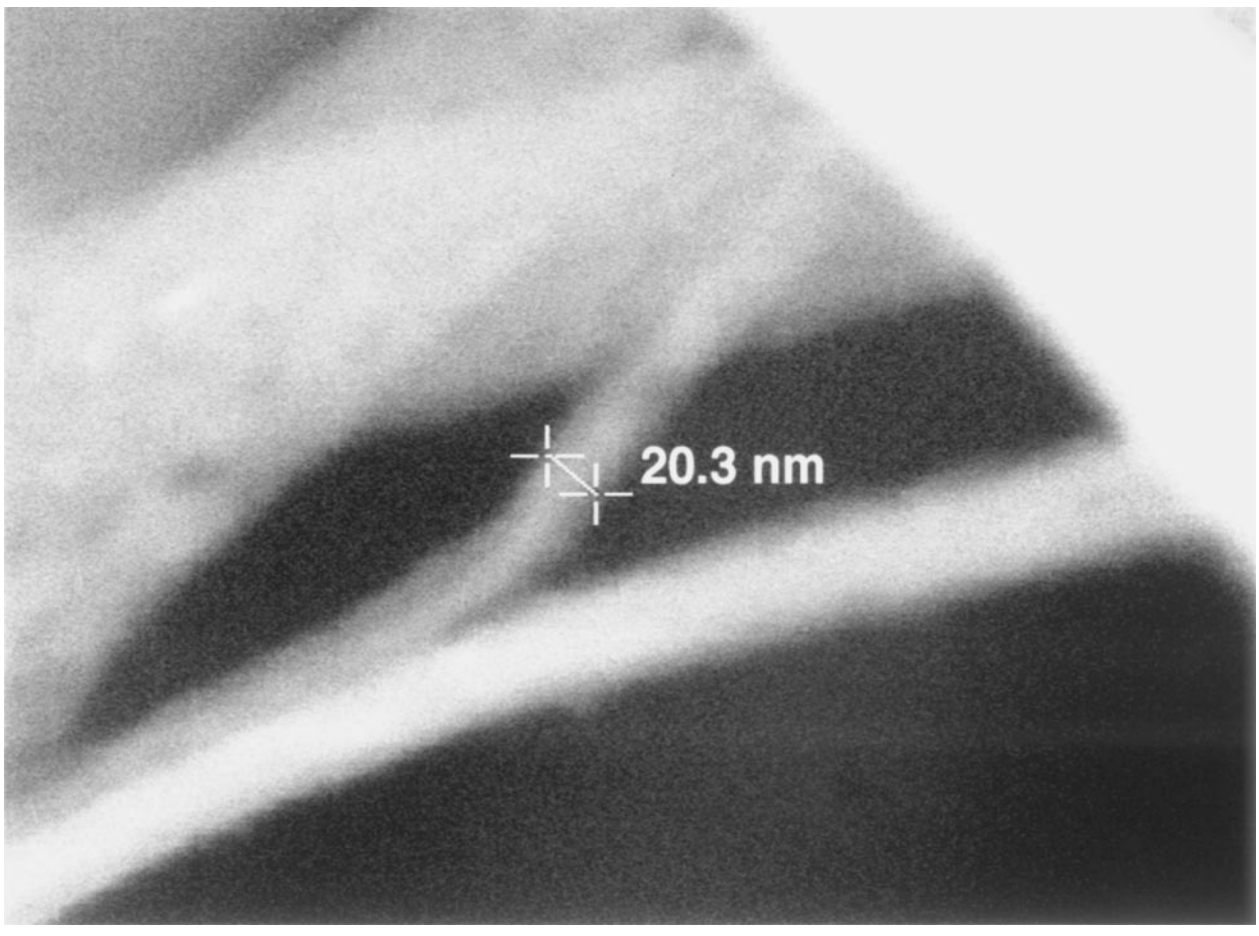

(b)

Figure 3 SEM micrographs of dysprosium ceramic fiber sample 2, a) at low magnification, b) at high magnification showing a fiber having a diameter of 20 nm. Nodules upon the surface of the fibers can also be discerned.

of a few hundred nanometers to a maximum of 1 micrometer, some fibers have diameters as small as 50 nm or less, as shown in Fig. 1c. The energy dispersive x-ray microanalysis of the fibers revealed the presence of dysprosium, fluorine and oxygen in the fibers. A TEM analysis of this sample confirmed this finding and further showed that the fibers have a single-crystal structure.

Fig. 2 presents an XRD scan from this sample. The closest structural match of the sample's major phase was obtained with yttrium hydroxide fluoride, a hexagonal crystal structure of the space group $P6_3/m$. (Note the reversed intensities of the doublet at 30 degrees) This finding suggests that the major phase is isomorphic to yttrium hydroxide fluoride with dysprosium substituting yttrium. However, it is important to note that from the XRD measurements alone we cannot resolve whether the oxygen is present in sample 1 as an oxide or as an hydroxide. The principle minor phase present in sample 1 was matched to a known standard having the composition $Dy_{1+x}O_{3x}F_{3(1-x)}$ [14]. This phase is also present in sample 2 that is described in the following paragraph.

Sample 2 was unexpectedly produced while conducting experiments (for ∼3 hours at 435°C, and 500 and 690 bar pressure) with a 0.2 m dysprosium bromide solution that contained an unknown amount of fluoride impurity. It is remarkable that this dysprosium sample survived at least 100 hours in various aqueous solutions (including $NiBr_2$) at temperatures exceeding 400°C without re-dissolving or aggregating into larger sized morphologies. Compared to sample 1, the SEM micrographs of sample 2 presented in Fig. 3 show fibers that are overall generally smaller in diameter. There are again also a number of platelet-like particles present. Both the platelets and fibers also contain dysprosium, fluorine and oxygen as determined from energy dispersive x-ray microanalysis. Although the fibers in sample 2 have similar dimensions they are not identical to the fibers in sample 1. Upon careful inspection of the high magnification micrograph shown in Fig. 3b one can discern nodules, in particular upon the two crossing 100 nm fibers located behind the 20 nm fiber in the upper left portion of Fig. 3b. These nodules are much more easily resolved in the TEM photograph shown in Fig. 4. During the inspection of the fiber shown in Fig. 4 by TEM, elemental analysis was completed on several nanometer-sized regions of the fiber. No change in the chemical composition (Dy, F, O) was found between the "lighter" or "darker" regions on and around the surface nodules. The fibers from sample 2 appeared to be less monolithic than the fibers in sample 1 but were also found to be crystalline. Only small amounts of sample 2 were available to obtain the lower quality XRD spectrum shown in Fig. 5. This XRD spectrum *does not* contain the hexagonal, yttrium hydroxide fluoride isomorphic phase that is the major phase in sample 1. Instead, the major phase in sample 2 is the $Dy_{1+x}O_{3x}F_{3(1-x)}$ phase that was also found as a minor phase in sample 1. The broad peaks are believed to be

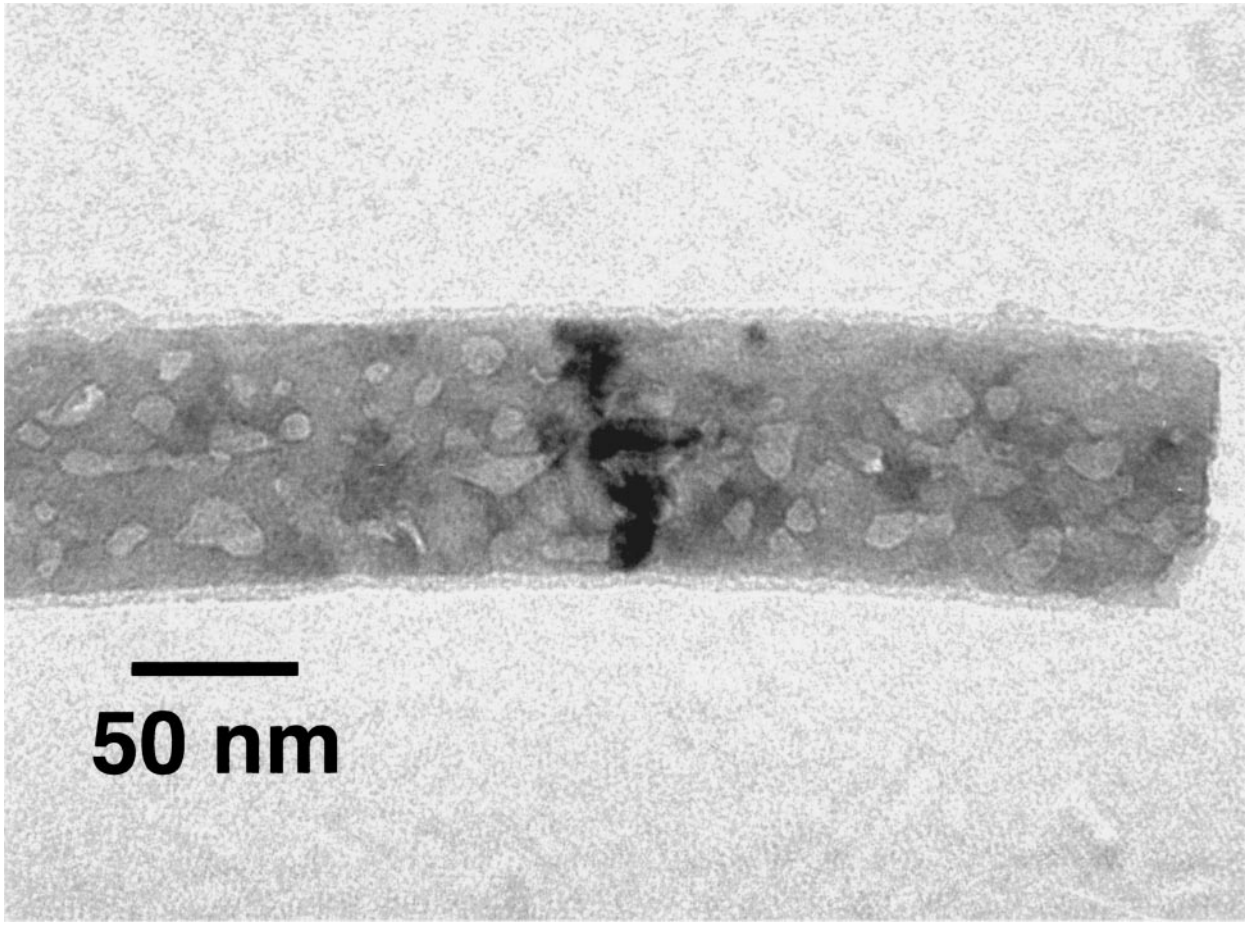

Figure 4 TEM micrograph of a single fiber from sample 2. The surface nodules present in this fiber are clearly visible.

due to a carbon-based adhesive from the sample support. Since the majority of the fibers present in sample 2 have diameters larger than 100 nm no broad lines are to be expected in the XRD from sample 2. It is conceivable that sample 2 dehydrated over the long (>100 hours) exposure to high-temperature water from a dysprosium hydroxide fluoride to a dysprosium oxofluoride.

3.2. Other observations

It is important to note that nano-sized dysprosium ceramic fibers cannot be produced from an aqueous solution of dysprosium bromide in the absence of fluoride. When a 0.2 molal $DyBr_3$ solution was introduced into the cell at 450°C and 515 bar and kept at these conditions for a prolonged time (17 hours), this did not result in the production of any dysprosium ceramic nano-fibers.

Another interesting observation is that the presence of other ions in the high-temperature dysprosium solutions can cause the formation of dysprosium compounds with very different morphologies. For instance, in Fig. 6 we show an SEM picture of large platelets that formed from an aqueous solution of dysprosium bromide *and* sodium tungstate that was kept at 450°C for a prolonged time. The platelets were found to contain oxygen combined with approximately equal amounts of dysprosium and tungsten.

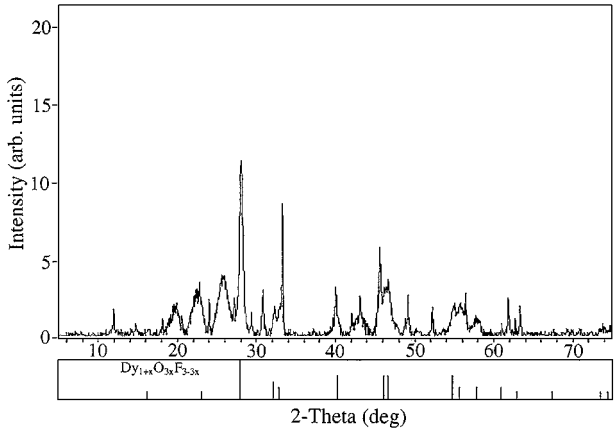

Figure 5 XRD plot of the major reflections of sample 2. The major phase is identified as $Dy_{1+x}O_{3x}F_{3(1-x)}$. The broad features are believed to be from a carbon based adhesive used to mount the small amount of sample.

3.3. Implications

The findings presented in the previous sections are unusual in many ways. To the best of our knowledge we know of no nano-structures of any kind that would form in a prolonged hydrothermal process at temperatures exceeding the critical temperature of pure water (374°C). At these high temperatures one would expect virtually no kinetic barriers to retard the growth rate. Typically, hydrothermal crystal growth results in much larger single crystals (like hydrothermal production of large synthetic quartz). It is also remarkable that the dysprosium ceramic nano-fibers are able to persist in

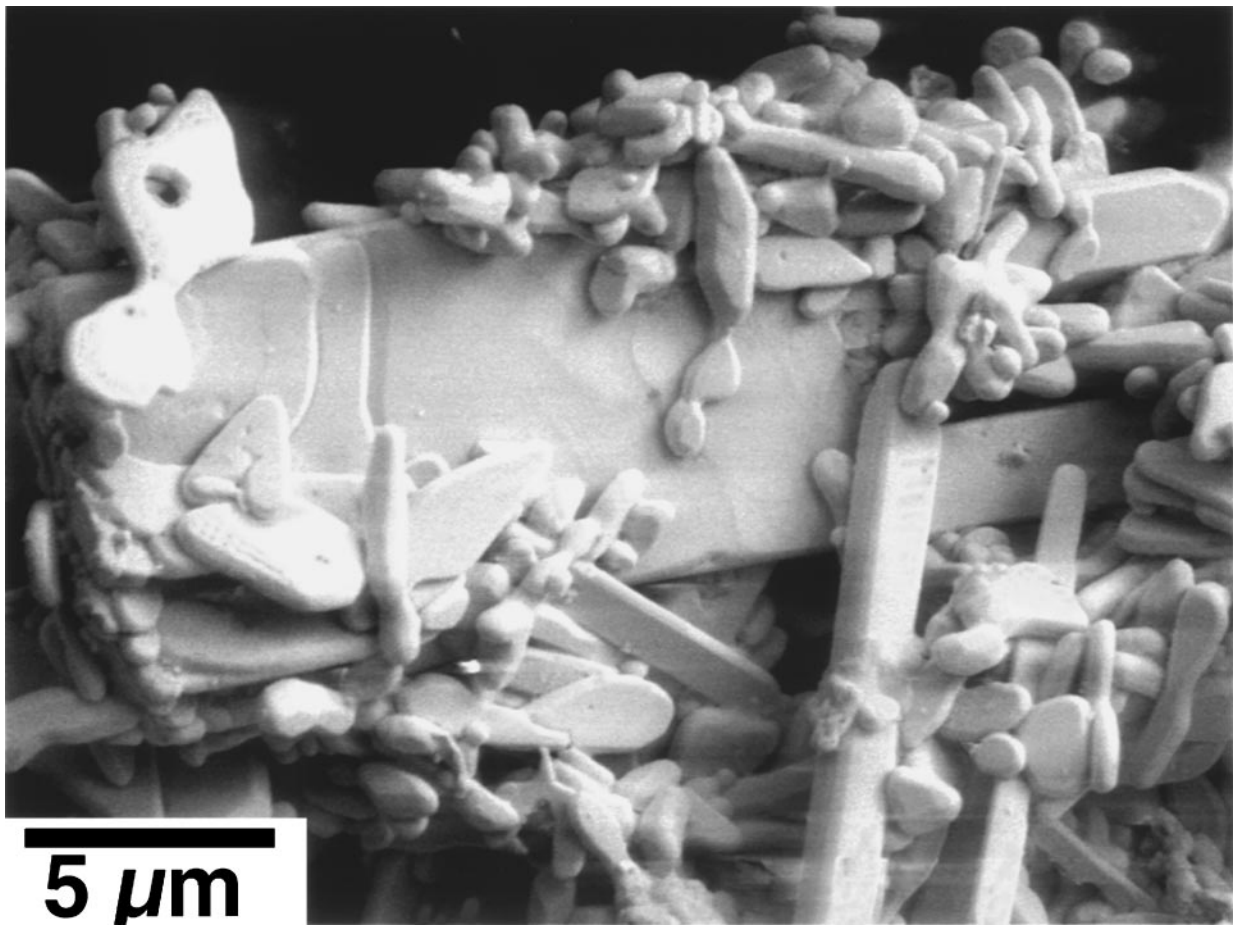

Figure 6 SEM micrograph of platelets containing Dy, W and O that were obtained from an aqueous solution of dysprosium bromide and sodium tungstate at 450°C.

these hydrothermal solutions over long time periods and in the particular case of sample 2, over a large range of temperatures as well.

Small filamentary single crystals with aspect ratios greater than 10 : 1 are known for their high strength which can approach the theoretical tensile strength of the crystal [15]. Due to their small structural dimensions, the new materials described in this report might be suitable as a high-strength material for fiber reinforcement of ceramic composites in applications at high temperatures and high stresses. Likewise, these materials may be used as a high surface-area support for catalytic compounds. In addition, because of the very low solubilities, these materials may be highly corrosion resistant to a range of high-temperature (supercritical) water solutions. Hence, this new material might find applications as a corrosion resistant coating in high-temperature aqueous solutions.

Finally, the rare-earth elements are known to be chemically very similar. Therefore, further work in this new area will include an exploration of the production of a variety of other rare-earth oxofluoride nano-fibers. This aspect may be of particular interest to the optical fiber industry that uses rare-earth-element-doped materials as optical amplifiers [16].

4. Conclusions

In summary, new materials consisting of dysprosium ceramic fibers with diameters as small as 20 nm were described that may be useful as high-strength material or as catalyst support material. The new materials were obtained from aqueous dysprosium bromide solutions under unusually high conditions of temperature and pressure. SEM, TEM and XRD analysis indicated that the fiber materials are crystalline dysprosium oxofluorides and/or dysprosium hydroxide fluorides. It is possible that other rare earth oxo/hydroxide fluorides may be obtained by similar methods as described here.

Acknowledgements

This research was supported by the Director, office of Energy Research, Office of Basic Energy Sciences, under contract No. DE-AC05-76RLO 1830. A portion of the research described in this paper was performed in the Environmental Molecular Sciences Laboratory, a national scientific user facility sponsored by the Department of Energy's Office of Biological and Environmental Research and located at Pacific Northwest National Laboratory, operated by Battelle Memorial Institute. The authors thank D. E. McCready, A. Jiricka and L. L. Davis for the expert XRD analysis as well as V. Y. Guertsman and J. S. Vetrano for the TEM analysis.

References

1. D. W. MATSON, J. L. FULTON, R. C. PETERSEN and R. D. SMITH, *Ind. Eng. Chem. Res.* **26** (1987) 2298.
2. D. M. MATSON, R. C. PETERSEN and R. D. SMITH, *J. Mat. Sci.* **22** (1987) 1919.
3. D. W. MATSON, J. C. LINEHAN and R. M. BEAN, *Mat. Lett.* **14** (1992) 222.
4. T. ADSCHIRI, K. KANAZAWA and K. ARAI, *J. Am. Ceram. Soc.* **75** (1992) 1019.
5. J. G. DARAB and D. W. MATSON, *J. Electronic Material*, **27** (1998) 1068.
6. D. W. MATSON, J. G. DARAB, T. D. BREWER and P. D. KAVIRATNA, *Mat. Res. Soc. Symp. Proc.* **520** (1998) 287.
7. J. G. DARAB, *Mat. Res. Soc. Symp. Proc.* **520** (1998) 161.
8. W. J. DAWSON, *Ceramic Bulletin* **67** (1988) 1673.
9. X. WANG, Y. WANG and J. ZHIHAO, *Xiyou Jinshu Cailiao Yo Gongcheng* **24** (1995) 1.
10. T. OOTA, J. SAITO and I. YAMAI, *J. Crystal Growth* **46** (1979) 331.
11. H. IZAWA, S. KIKKAWA and M. KOIZUMI, *Funtai oyobi Funmatsu Yakin* **33** (1986) 353.
12. A. D. FEDOSEEV, T. A. MAKAROVA, N. I. NESTERCUK and D. P. SIPOVSKIJ, *Kristall und Technik* **3** (1968) 95.
13. M. YOSHIMURA, H. SUDA, K. OKAMOTO and K. IOKU, *J. Mater. Sci.* **29** (1994) 3399.
14. A. DE KOZAK, M. SAMOUËL and A. ERB, *Rev. Chim. Miner.* **17** (1980) 440.
15. S. JAGOTA and R. RAJ, *J. Crystal Growth* **85** (1987) 527.
16. P. M. BRIDENBAUGH, J. O. ECKERT, G. NYKOLAK, G. THOMAS, W. WILSON, L. M. DEMIANETS, R. RIMAN and R. A. LAUDISE, *J. Crystal Growth* **144** (1994) 243.

Received 5 May 1999
and accepted 8 February 2000